Beam Tracking Method Using Unscented Kalman Filter for UAV-Enabled NR MIMO-OFDM System with Hybrid Beamforming

Yuna Sim[1], Seungseok Sin[2], Jihun Cho[3], Sangmi Moon[4], Young-Hwan You[5], Cheol Hong Kim[6] , and Intae Hwang[7*]

[1] Department of ICT Convergence System Engineering, Chonnam National University,
77, Yongbong-ro, Buk-gu, Gwangju, 61186, Republic of Korea
[e-mail: sya8325@naver.com]
[2] School of Electronics and Computer Engineering, Chonnam National University,
77, Yongbong-ro, Buk-gu, Gwangju, 61186, Republic of Korea
[e-mail: ssskit7@naver.com]
[3] Department of ICT Convergence System Engineering, Chonnam National University,
77, Yongbong-ro, Buk-gu, Gwangju, 61186, Republic of Korea
[e-mail: hoony1992@naver.com]
[4] Department of IT Artificial Intelligence, Korea Nazarene University,
Wolbong-ro 48, Cheonan-city, Choongcheongnam-do, 31172, Republic of Korea
[e-mail: moonsm@kornu.ac.kr]
[5] Department of Computer Engineering, Sejong University
209, Neungdong-ro, Gwangjin-gu, Seoul, 05006, Republic of Korea
[e-mail: yhyou@sejong.ac.kr]
[6] School of Computer Science and Engineering, Soongsil University,
369 Sangdo-Ro, Dongjak-Gu, Seoul, 06978, Republic of Korea
[e-mail: cheolhong@ssu.ac.kr]
[7] Department of Electronic Engineering and Department of ICT Convergence System Engineering,
College of Engineering, Chonnam National University,
77, Yongbong-ro, Buk-gu, Gwangju, 61186, Republic of Korea
[e-mail: hit@jnu.ac.kr]
[*]Corresponding author: Intae Hwang

Received October 10, 2022; revised January 9, 2023; accepted January 18, 2023; published January 31, 2023

Abstract

Unmanned aerial vehicles (UAVs) and millimeter-wave frequencies play key roles in supporting 5G wireless communication systems. They expand the field of wireless communication by increasing the data capacities of communication systems and supporting

"This work was supported by the National Research Foundation of Korea (NRF) grant funded by the Korea government(MSIT: Ministry of Science and ICT) (2020R1I1A1A01073948 and 2021R1A2C1005058)." "This research was supported by the BK21 Fostering Outstanding Universities for Research (FOUR) Program (5199991714138) funded by the Ministry of Education (MOE, Korea) and National Research Foundation of Korea (NRF). " "This research was supported by the Ministry of Science and ICT (MSIT), Korea, under the Innovative Human Resource Development for Local Intellectualization support program (IITP-2022-RS-2022-00156287) supervised by the Institute for Information & communications Technology Planning & Evaluation (IITP). " “This research was supported by the Ministry of Science and ICT (MSIT), Korea, under the ICT Challenge and Advanced Network of HRD (ICAN) program (IITP-2022-RS-2022-00156385) supervised by the Institute of Information & communications Technology Planning & Evaluation (IITP).”.

high data rates. However, short wavelengths, owing to the high millimeter-wave frequencies can cause problems, such as signal attenuation and path loss. To address these limitations, research on high directional beamforming technologies continue to garner interest. Furthermore, owing to the mobility of the UAVs, it is essential to track the beam angle accurately to obtain full beamforming gain. This study presents a beam tracking method based on the unscented Kalman filter using hybrid beamforming. The simulation results reveal that the proposed beam tracking scheme improves the overall performance in terms of the mean-squared error and spectral efficiency. In addition, by expanding analog beamforming to hybrid beamforming, the proposed algorithm can be used even in multi-user and multi-stream environments to increase data capacity, thereby increasing utilization in new-radio multiple-input multiple-output orthogonal frequency-division multiplexing systems.

Keywords: Beam tracking, hybrid beamforming, multiple-input multiple-output, orthogonal frequency diversity multiplexing, unscented Kalman filter.

1. Introduction

In new-radio multiple-input multiple-output orthogonal frequency-division multiplexing (NR MIMO-OFDM) systems, the use of unmanned aerial vehicles (UAVs) is increasingly attracting attention as they play crucial roles in 5G NR systems because of their high-altitude, flexibility, and mobility characteristics. Various types of UAVs are currently used in different situations. For example, a high-level UAV platform can extend the range of the radio area to be serviced, whereas a relatively low-level platform can help easily access time-sensitive systems. In addition, in hotspot areas where network usage is increasing rapidly, if the data capacity can be increased using a UAV as the base station (BS), the problems of excess data traffic can be solved [1,2]. The massive multiple-input multiple-output (m-MIMO) technology, which increases data transmission and reception efficiency through multiple antennas, is also a promising approach that supports high data rates in NR MIMO-OFDM systems [3]. Moreover, if UAVs and millimeter-wave frequencies can be integrated into NR MIMO-OFDM systems, the wireless communication area coverage can be expanded by increasing the data capacity, thus enabling high transmission speeds of 5G systems.

However, short wavelengths resulting from high millimeter-wave frequencies can cause problems, such as signal attenuation and path loss. To overcome these drawbacks, researchers have increasingly focused on high-directionality beamforming techniques. Given the full beamforming gain and high mobility of UAVs, it is essential to obtain accurate beam angles. Furthermore, accurate beam tracking techniques are essential in UAV-enabled NR MIMO-OFDM systems. Therefore, in this study, we propose an unscented Kalman filter (UKF)-based beam tracking method using hybrid beamforming.

The remainder of the paper is structured as follows. Chapter II introduces the channel model that will be defined and applied with the system model. Chapter III introduces the UKF-based beam tracking method using hybrid beamforming, and Chapter IV presents performance evaluations through simulations and their results. Finally, Chapter V presents the conclusions of this study.

2. System Model and Channel Model

2.1 System Model

In this study, we considered a downlink UAV-enabled NR MIMO-OFDM system where a UAV-BS served as the ground-user equipment (G-UE).

Both the transmitter-side UAV-BS and receiver-side G-UE had antenna arrays in the form of a uniform planar array (UPA) placed evenly on the xy-plane, as shown in **Fig. 1**. The UAV-BS and G-UE had UPAs of $M_t \times N_t$ each. The spacing between the adjacent antennas was uniformly $d\ (=\lambda/2)$, $d = d_H = d_V$, with d_H being in the horizontal-axis direction and d_V being in the vertical-axis direction. The carrier wavelength is denoted by λ.

The zenith and azimuth angles in the transmitter are denoted by θ_t (zenith angle of departure, ZOD) and ϕ_t (azimuth angle of departure, AOD), respectively, and the corresponding angles in the receiver are denoted by θ_r (zenith angle of arrival, ZOA) and ϕ_r (azimuth angle of arrival, AOA), respectively. The angle notations follow the definitions specified in the 3GPP TR 38.901 v16.1.0 [4].

The beamformer and combiner vectors are given by $\boldsymbol{v}_k$ ($\boldsymbol{v}_k \in C^{(M_t N_t)\times 1}$) and $\boldsymbol{w}_k$ ($\boldsymbol{w}_k \in C^{(M_r N_r)\times 1}$), respectively. When a transmission signal x_k is transmitted, the received signal is given by (1). The notation $\boldsymbol{h}_k$ ($\boldsymbol{h}_k \in C^{(M_t N_t)\times(M_r N_r)}$) represents a 3D channel between the UAV-BS and G-UE in the k^{th} transmission time interval (TTI). Moreover, n_k is additive white Gaussian noise that follows a normal distribution given by $n_k \sim N(0, \sigma_n^2)$ and is applied in the k^{th} TTI.

$$y_k = \boldsymbol{w}_k^H \boldsymbol{h}_k^H \boldsymbol{v}_k x_k + n_k. \tag{1}$$

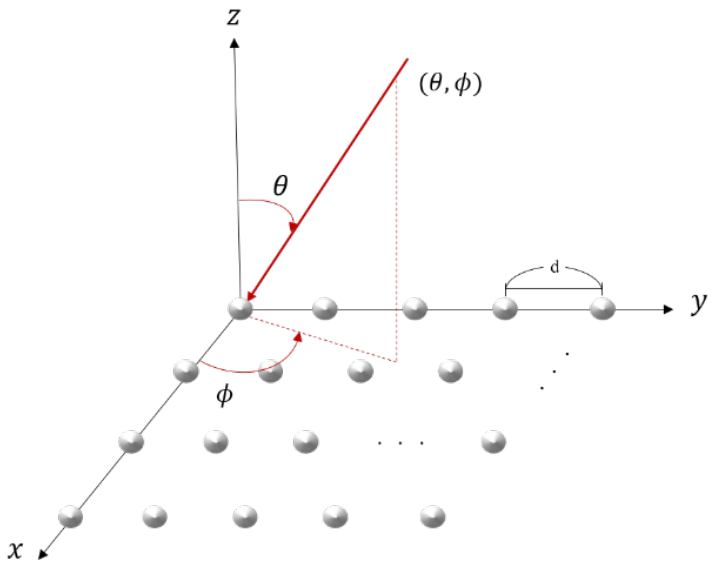

Fig. 1. Uniform planar antenna array used for the transmitter and receiver.

2.2 Channel Model

In the NR MIMO-OFDM communication system proposed herein, we considered a slow-varying channel model where the channels did not change within a given TTI but did between TTIs [5]. However, this cannot explain the rapid movement of the UAV, so finding another beam tracking method by considering this characteristic will be a future research task. We express the L_k-scatterer channel model in (2) by applying the antenna array response vector $(\boldsymbol{a}(\theta_{l,k},\ \phi_{l,k}))$ at the transmitter and receiver sides. Here, the path gain is represented by $\eta_{l,k}$ and is calculated using (3). Further, the attenuation degree of the signal is $\rho_{l,k}$, and d_l represents the distance between the transmit antenna and receive antenna along the path l, as shown in **Fig. 1**. The antenna array response vectors of the uniform square planar array configurations of both the transmitter and receiver can be modeled as shown in (4) [6]. Here, the antenna indexes of the elements along the horizontal and vertical axes in the antenna array are represented as $m\ (0 < m < M-1)$ and $n\ (0 < n < N-1)$, respectively, and the total number of antennas is MN.

$$\boldsymbol{h}_k = \sum_{l=1}^{L_k} \eta_{l,k} \boldsymbol{a}_r^H(\theta_{l,k}^r, \phi_{l,k}^r) \boldsymbol{a}_t(\theta_{l,k}^t, \phi_{l,k}^t), \tag{2}$$

$$\eta_{l,k} = \rho_{l,k}\sqrt{M_r N_r M_t N_t}\, e^{-j\frac{2\pi d_l}{\lambda}}, \tag{3}$$

$$a(\theta,\phi) = \frac{1}{\sqrt{MN}}\left(\left[1, \ldots, e^{jkd(m\sin(\theta)\sin(\phi)+n\sin(\theta)cos(\phi)}, \ldots, e^{jkd((M-1)\sin(\theta)\sin(\phi)+(N-1)\sin(\theta)cos(\phi)}\right]\right)^T. \tag{4}$$

However, most millimeter-wave frequency signals cause signal losses owing to obstacles, such as buildings and people. Consequently, most of the signal power transmitted from the UAV-BS to the G-UE is from the line-of-sight (LOS) path [7, 8]. Therefore, in the UAV-enabled NR MIMO-OFDM proposed in this study, only the LOS path was considered. The channel vector can be expressed as in (5), where the variables have the same meanings as noted previously.

$$\boldsymbol{h}_k = \eta_k \boldsymbol{a}_r^H(\theta_k^r, \phi_k^r) \boldsymbol{a}_t(\theta_k^t, \phi_k^t), \tag{5}$$

3. UKF-Based Beam Tracking Using Hybrid Beamforming

Owing to the short wavelengths of millimeter-wave frequencies and the high mobility of the UAV, it is imperative to obtain the exact beam angle. This section presents a method for tracking the beam angle based on the UKF using hybrid beamforming.

3.1 Hybrid Beamforming

Beamforming is a technology that allows multiple antennas to be arranged at regular intervals to create an antenna beam in a specific direction by changing the amplitude and phase of the signal supplied through each antenna to transmit and receive strong signals. In particular, in the case of 5G systems that use high-frequency millimeter waves, the wavelength is small; thus, the separation between antennas can also be reduced, enabling integration of m-MIMO technology in antennas with high densities. Therefore, the application of beamforming techniques through square planar antenna arrays to the NR MIMO-OFDM system in this study

can lead to expanded cell coverage and increased transmission speeds.

Beamforming technologies can be divided into analog, fully digital, and hybrid beamforming. Analog beamforming involves the application of a beam generator to the radio frequency (RF) stage. This method has a relatively low implementation complexity, but it is difficult to implement an arbitrary beamforming matrix. Further, it has the disadvantage of being limited to one user and a single transmission and reception flow. In the case of fully digital beamforming, the beamforming generators are applied to the baseband. Beamforming can be applied by allocating different frequency resources to each user in the cell, thus forming a beam for multiple users simultaneously. In addition, an arbitrary beamforming matrix can be implemented using digital signal processing to facilitate interference and power control between the users. However, implementing this method consumes extensive hardware resources. It also has the limitation of high processing complexity. Therefore, in this study, we used hybrid beamforming to apply beam generators to both the RF stage and baseband. In other words, we used analog and electronic beamforming simultaneously.

The hybrid precoding structure applied in this study is shown in **Fig. 2** [9]. Digital precoding was performed using $\boldsymbol{V}_{BB}$ ($\boldsymbol{V}_{BB} \in C^{N_T^{RF} \times N_s}$) by the data symbols, $\boldsymbol{N}_s$ in the transmitter. Thereafter, a cyclic prefix (CP) was inserted after converting to time domain through the K-point inverse fast Fourier transform (IFFT). Lastly, analog precoding was applied using $\boldsymbol{V}_{RF}$ ($\boldsymbol{V}_{RF} \in C^{N_T \times N_T^{RF}}$) and transmitted to the channel.

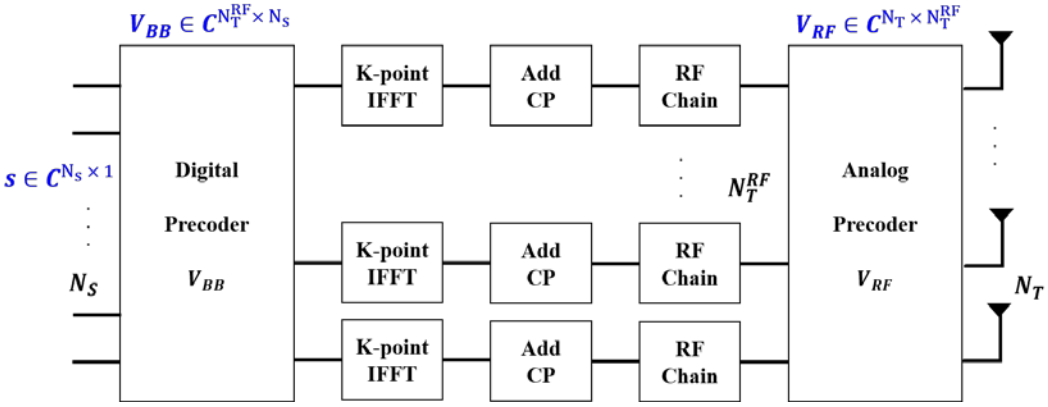

Fig. 2. Hybrid pre-coding structure.

3.2 UKF-Based Beam Tracking

This section introduces the UKF-based beam tracking scheme [10, 11]. In this study, the channel angle vector is defined as shown in (6); for convenience, this is called as a state vector. Here, the state vector variation equation follows (7), and $\boldsymbol{q}_k$ ($\boldsymbol{q}_k \in N^{4\times1}$) represents the Gaussian noise. Additionally, $\boldsymbol{q}_k$ follows the normal distribution $N(0, \boldsymbol{Q})$, and $\boldsymbol{Q}$ ($\boldsymbol{Q} = \sigma^2 \boldsymbol{I}_4$) is a 4×4 matrix of channel angle variance (σ^2) that indicates how fast the channel changes. In a real system, the channel angle variance depends on the ZOD(θ_k^t), AOD(ϕ_k^t), ZOA(θ_k^r), and AOA(ϕ_k^r). However, for computational convenience, we assumed the same values for these in the study

$$\boldsymbol{\psi}_k = [\theta_k^t \;\; \phi_k^t \;\; \theta_k^r \;\; \phi_k^r]^T, \tag{6}$$

$$\boldsymbol{\psi}_k = \boldsymbol{\psi}_{k-1} + \boldsymbol{q}_k, \tag{7}$$

The signal received by the proposed UKF-based beam tracking scheme is represented through (8). Since y_k and n_k are complex forms, (8) can be redefined as (9) and (10). The nonlinear measurement function is expressed using $f(\boldsymbol{\psi}_k)$ and $g(\boldsymbol{\psi}_k)$, as shown in (11).

$$y_k = \boldsymbol{w}_k^H \boldsymbol{h}_k^H \boldsymbol{v}_k x_k + n_k = \eta_k \boldsymbol{w}_k^H \boldsymbol{a}_r(\theta_k^r, \phi_k^r) \boldsymbol{a}_t^H(\theta_k^t, \phi_k^t) \boldsymbol{v}_k x_k + n_k, \tag{8}$$

$$y_k = \begin{bmatrix} Re(y_k) \\ Im(y_k) \end{bmatrix} = \begin{bmatrix} Re(\boldsymbol{w}_k^H \boldsymbol{h}_k^H \boldsymbol{v}_k x_k + n_k) \\ Im(\boldsymbol{w}_k^H \boldsymbol{h}_k^H \boldsymbol{v}_k x_k + n_k) \end{bmatrix}, \tag{9}$$

$$\begin{gathered} \boldsymbol{n}_k = [Re(n_k)\ Im(n_k)]^T, \\ \boldsymbol{n}_k \sim N(0,\ \boldsymbol{Q}_n), \\ \boldsymbol{Q}_n = \frac{\sigma_n^2}{2} \boldsymbol{I}_2, \end{gathered} \tag{10}$$

$$\begin{aligned} f(\boldsymbol{\psi}_k) &= Re\left(\boldsymbol{w}_k^H \boldsymbol{h}_k^H \boldsymbol{v}_k x_k\right), \\ g(\boldsymbol{\psi}_k) &= Re\left(\boldsymbol{w}_k^H \boldsymbol{h}_k^H \boldsymbol{v}_k x_k\right), \end{aligned} \tag{11}$$

The initial state vector and covariance were calculated using (12) and (13):

$$\widehat{\boldsymbol{\psi}}_0 = E[\boldsymbol{\psi}], \tag{12}$$

$$\boldsymbol{P}_0 = E[(\boldsymbol{\psi} - \widehat{\boldsymbol{\psi}}_0)(\boldsymbol{\psi} - \widehat{\boldsymbol{\psi}}_0)^T], \tag{13}$$

To predict the next state vector, the previous state vector was used. Therefore, the state vector and covariance were predicted using (14) and (15), respectively. Here, the state index is represented as k, which is an integer greater than or equal to 1.

$$\widehat{\boldsymbol{\psi}}_k^f = \widehat{\boldsymbol{\psi}}_{k-1}, \tag{14}$$

$$\overline{\boldsymbol{P}}_k = \boldsymbol{P}_{k-1} + \boldsymbol{Q}_g, \tag{15}$$

The UKF-based beam tracking method proposed herein tracks angles by estimating the motion state of the UAV as a Gaussian distribution by substituting several sample points called sigma points into a nonlinear measurement function.

Here, $\overline{\boldsymbol{\psi}}_k$ represents the $(2n + 1)$ sigma points, as shown in (16), where the value of n is 4, the dimension of the state vector, as shown in (6).

$$\overline{\boldsymbol{\psi}}_k = [\overline{\boldsymbol{\psi}}_k^0\ \ \overline{\boldsymbol{\psi}}_k^1\ \ \ldots\ \ \overline{\boldsymbol{\psi}}_k^{2n+1}], \tag{16}$$

Each element of $\overline{\boldsymbol{\psi}}_k$ can be calculated through (17). Here, the i-th column vector of the matrix shown in (15) is represented as $(\sqrt{\overline{P}_k})_{(i)}$, and the weights in (17) can be calculated through (18). Here, s is a scaling variable, and α is a constant indicating the degree to which the sigma points are spread around the predicted state vector ($\widehat{\boldsymbol{\psi}}_k^f$). Here, the constant α is usually set to a small positive value within the range $10^{-4} \leq \alpha \leq 1$ and was calculated as 10^{-3} in this study. The constant κ represents a quadratic scaling variable and was calculated as $(3 - n)$.

$$\begin{aligned} \bar{\boldsymbol{\psi}}_k^0 &= \hat{\boldsymbol{\psi}}_k^f, \\ \bar{\boldsymbol{\psi}}_k^i &= \hat{\boldsymbol{\psi}}_k^f + \gamma\left(\sqrt{\bar{P}_k}\right)_{(i)}, i = 1, \dots, n, \\ \bar{\boldsymbol{\psi}}_k^i &= \hat{\boldsymbol{\psi}}_k^f - \gamma\left(\sqrt{\bar{P}_k}\right)_{(i)}, i = n+1, \dots, 2n, \end{aligned} \tag{17}$$

$$\begin{aligned} \gamma &= \sqrt{n+s}, \\ s &= \alpha^2(n+\kappa) - n, \end{aligned} \tag{18}$$

As in the process of (19), the previously calculated sigma points were substituted into the non-linear measurement function, and the result is expressed as $\boldsymbol{Z}_k$ ($\boldsymbol{Z}_k = [Z_k^0 \ Z_k^1 \ \dots \ Z_k^{2n+1}]^T$).

$$Z_k^i = [f(\bar{\boldsymbol{\psi}}_k) \ \ g(\bar{\boldsymbol{\psi}}_k)]^T, i = 0, \dots, 2n, \tag{19}$$

The state vector and auto-covariance can be estimated from the Gaussian distribution using the output value (Z_k^i) of the nonlinear measurement function. (20) represents the process of estimating the state vector, and (21) shows the process of estimating the auto-covariance. The weights used for each calculation are expressed in (22). When estimating the distribution of the state vector ($\boldsymbol{\psi}$), the value β was set to 2 because the estimated distribution followed a Gaussian distribution.

$$\hat{\boldsymbol{Z}}_k = \sum_{i=0}^{2n} W_i^m Z_k^i, \tag{20}$$

$$\boldsymbol{P}_{(ZZ)k} = \sum_{i=0}^{2n} W_i^c [Z_k^i - \hat{\boldsymbol{Z}}_k][Z_k^i - \hat{\boldsymbol{Z}}_k]^T + \boldsymbol{Q}_n, \tag{21}$$

$$\begin{aligned} W_0^m &= \frac{s}{n+s}, \\ W_0^c &= \frac{s}{n+s} + (1 - \alpha^2 + \beta), \\ W_i^m &= W_i^c = \frac{s}{2(n+s)}, i = 1, \dots, 2n, \end{aligned} \tag{22}$$

The cross-covariance between the state vector ($\hat{\boldsymbol{\psi}}_k^f$) previously predicted through (14) and state vector ($\hat{\boldsymbol{Z}}_k$) estimated through (20) can be calculated using (23).

$$\boldsymbol{P}_{(XZ)k} = \sum_{i=0}^{2n} W_i^c [\bar{\boldsymbol{\psi}}_k^i - \hat{\boldsymbol{\psi}}_k^f][Z_k^i - \hat{\boldsymbol{Z}}_k]^T, \tag{23}$$

The UKF Kalman gain (ε_k) can be calculated using (24) with the previously calculated auto-covariance ($\boldsymbol{P}_{(ZZ)k}$) and cross-covariance ($\boldsymbol{P}_{(XZ)k}$). Additionally, using the calculated Kalman gain values, we modified the state vector ($\hat{\boldsymbol{\psi}}_k^f$) and covariance ($\bar{\boldsymbol{P}}_k$) predicted in (14) and (15). (25) denotes the final estimate of the current channel angle vector ($\hat{\boldsymbol{\psi}}_k$), and (26) represents the final covariance of the channel angle vector ($\boldsymbol{P}_k$). Both values were used for beam tracking in the following state. The UKF-based beam tracking scheme is summarized in the flow chart in **Fig. 3**.

$$\varepsilon_k = \boldsymbol{P}_{(XZ)k} \boldsymbol{P}_{(ZZ)k}^{-1}, \tag{24}$$

$$\hat{\boldsymbol{\psi}}_k = \hat{\boldsymbol{\psi}}_k^f + \varepsilon_k [\boldsymbol{Z}_k - \hat{\boldsymbol{Z}}_k], \tag{25}$$

$$\boldsymbol{P}_k = \bar{\boldsymbol{P}}_k - \varepsilon_k \boldsymbol{P}_{(ZZ)k} \varepsilon_k^T. \tag{26}$$

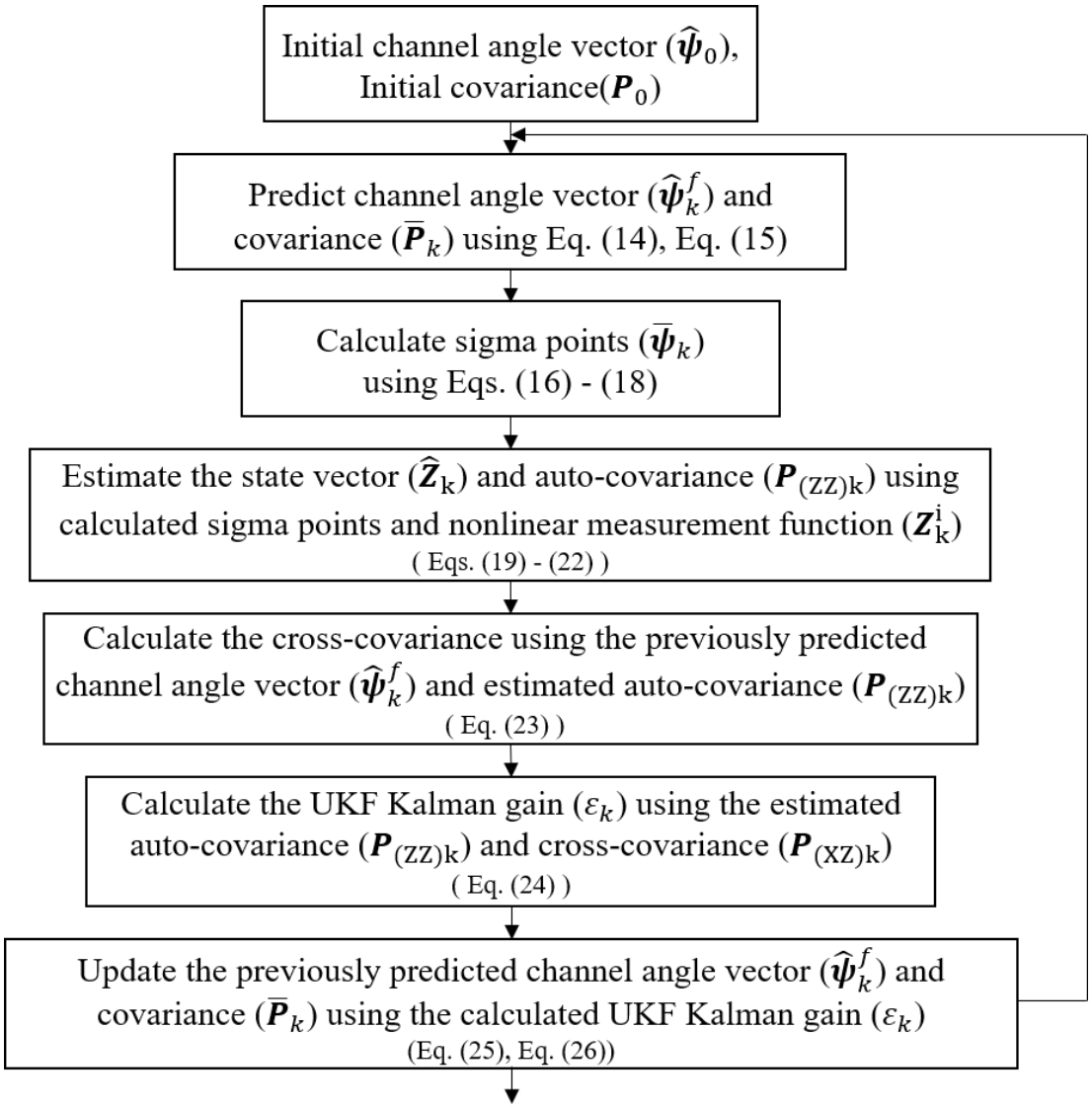

Fig. 3. UKF-based beam tracking algorithm using hybrid beamforming.

4. Simulation Results

In this section, we present and analyze the simulation results. The simulation environment and results are as follows.

4.1 Simulation Setup

Table 1 outlines the simulation system parameters. The simulations were performed based on the UAV-enabled NR downlink MIMO-OFDM system, which was configured to have a system bandwidth of 100 MHz in the frequency band of 30 GHz.

Table 1. System parameters

Parameter	Values
Carrier frequency (GHz)	30
System bandwidth (MHz)	100
Sub-carrier spacing (kHz)	60
Modulation/demodulation method	QPSK
UAV-BS antenna configuration	UPA : 16 × 16
G-UE antenna configuration	UPA : 4× 4
Number of RF chains	8 / 16
Antenna spacing	0.5
Initial ZOD/AOD/ZOA/AOA	$\frac{\pi}{4}$
Number of streams	1

4.2 Performance Evaluation

An existing work on comparative analysis proposes a UKF-based beam tracking technique using analog beamforming [11], so our study compares and analyzes the case of using analog and hybrid beamforming to evaluate the performance improvement by the proposed technique. The mean square error (MSE), frame error rate (FER), throughput, and spectral efficiency (SE) were used as the performance indicators. In addition, all the performance indicators were based on AOD. In the case of MSE, it was calculated using (26). Because the remaining ZOD, AOA, and ZOA showed similar patterns to the AOD, only the AOD components have been covered in this study.

$$MSE = E[|\phi_k^t - \hat{\phi}_k^t|^2]. \tag{27}$$

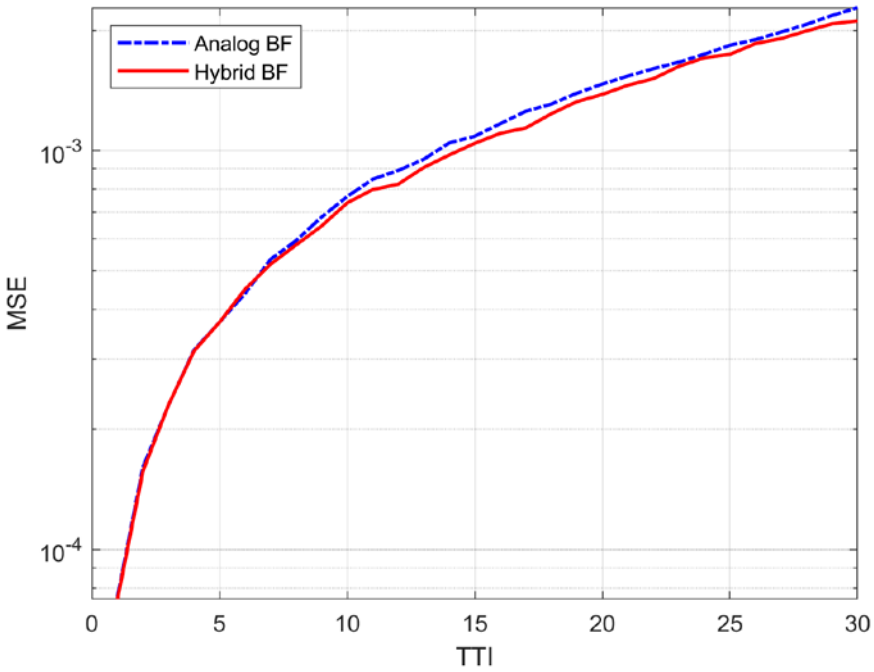

Fig. 4. Comparison of beam tracking performances based on the UKF according to beamforming type (MSE).

Fig. 4 shows the simulation results and comparison of the performances with respect to MSE based on the beamforming type. When the UKF-based beam tracking was performed using hybrid beamforming, it was found that the MSE improved to a greater extent than when analog beamforming was used.

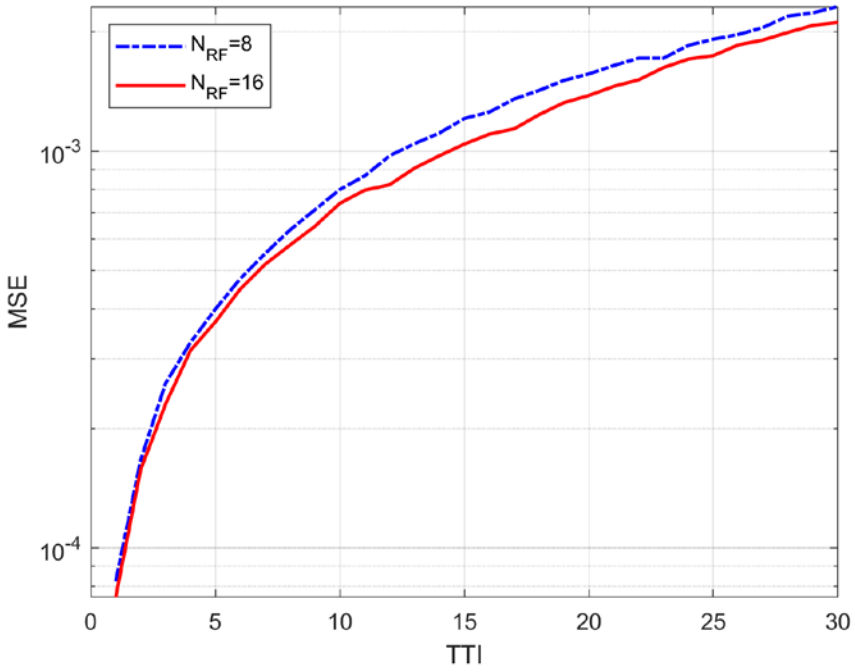

Fig. 5. Comparison of beam tracking performances based on the UKF according to the number of RF chains (MSE).

Fig. 5 shows the simulation results for comparison of the MSE performances according to the number of RF chains when using hybrid beamforming. The simulations were conducted for 8 and 16 RF chains. As seen in **Fig. 5**, the performance was improved when the number of RF chains was 16 instead of 8. Thus, in the following simulations, when hybrid beamforming was used, the experiments were conducted with 16 RF chains.

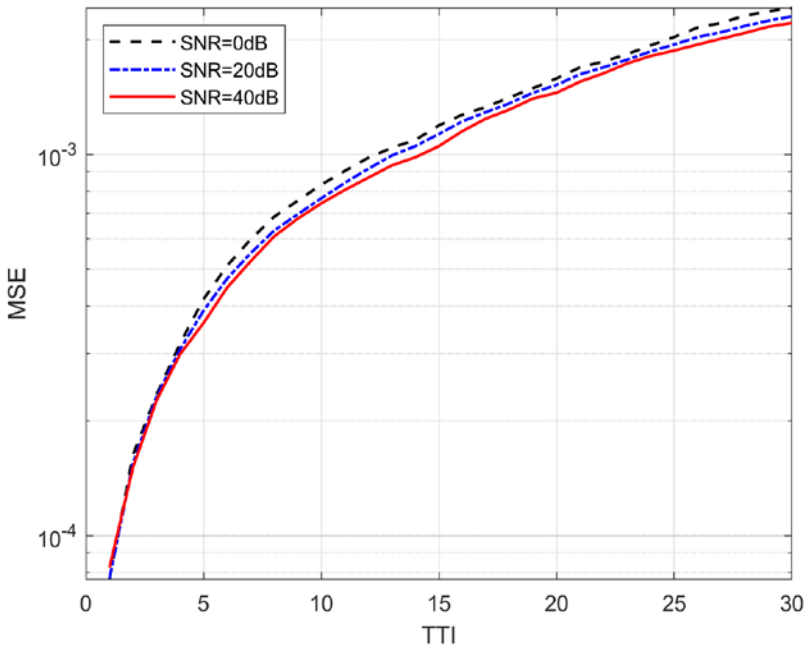

Fig. 6. Comparison of beam tracking performances based on the UKF according to signal-to-noise ratio (SNR) (MSE).

Fig. 6 shows the results of analyzing the MSE performances of the UKF-based beam tracking algorithm when using hybrid beamforming at different signal-to-noise ratios (SNRs). As the SNR increased, the estimated MSE of the AOD gradually decreased. In this case, the channel angle variance (σ^2) was set to $(0.5°)^2$ to perform the simulations.

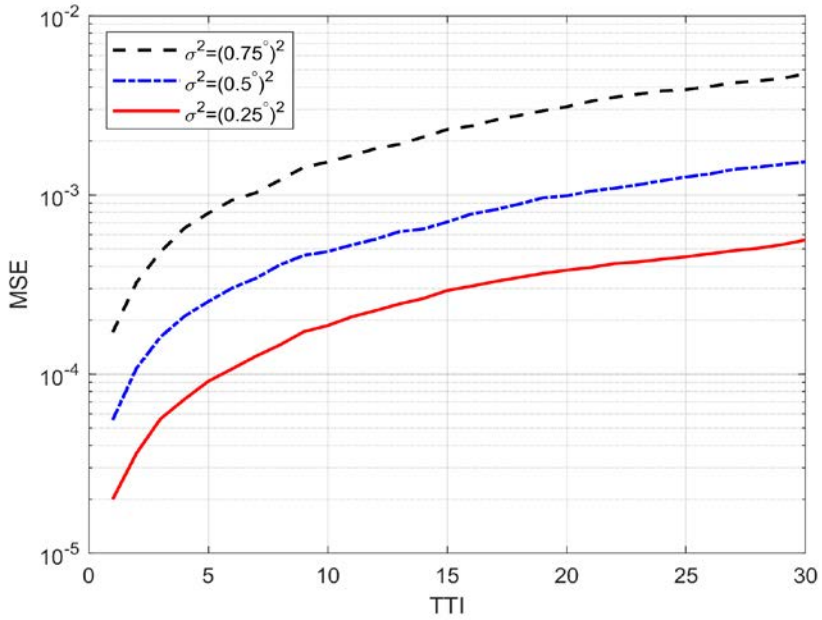

Fig. 7. Comparison of beam tracking performances based on the UKF according to the channel angle variance (MSE).

Fig. 7 shows the simulation results of analyzing the MSE performance of the proposed algorithm according to channel angle variance (σ^2). As the value of the channel angle variance increased, the channel changed rapidly and beam tracking based on the UKF became difficult. Consequently, as can be seen in **Fig. 7**, the MSE of the AOD increased. The SNR was set to 20 dB.

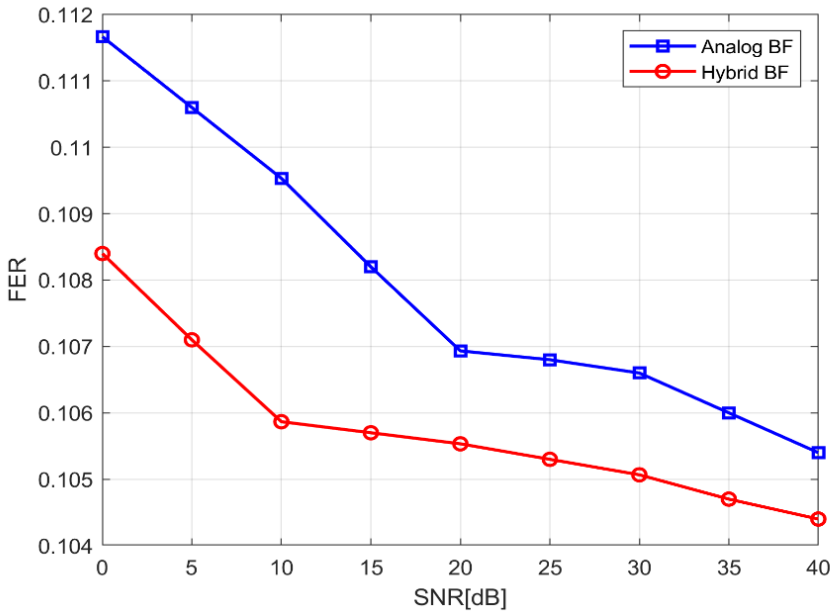

Fig. 8. Comparison of beam tracking performances based on the UKF according to the beamforming type (FER).

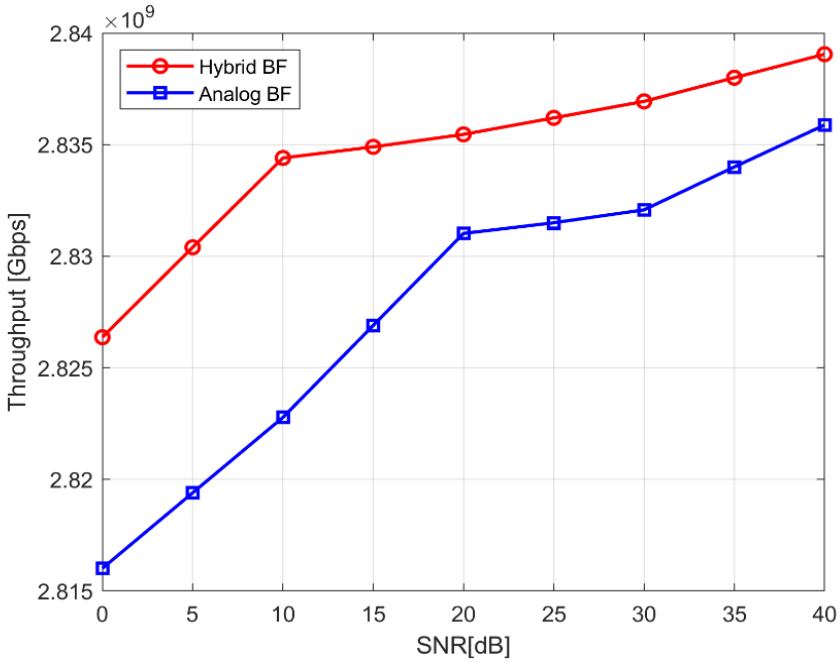

Fig. 9. Comparison of beam tracking performances based on the UKF according to the beamforming type (Throughput).

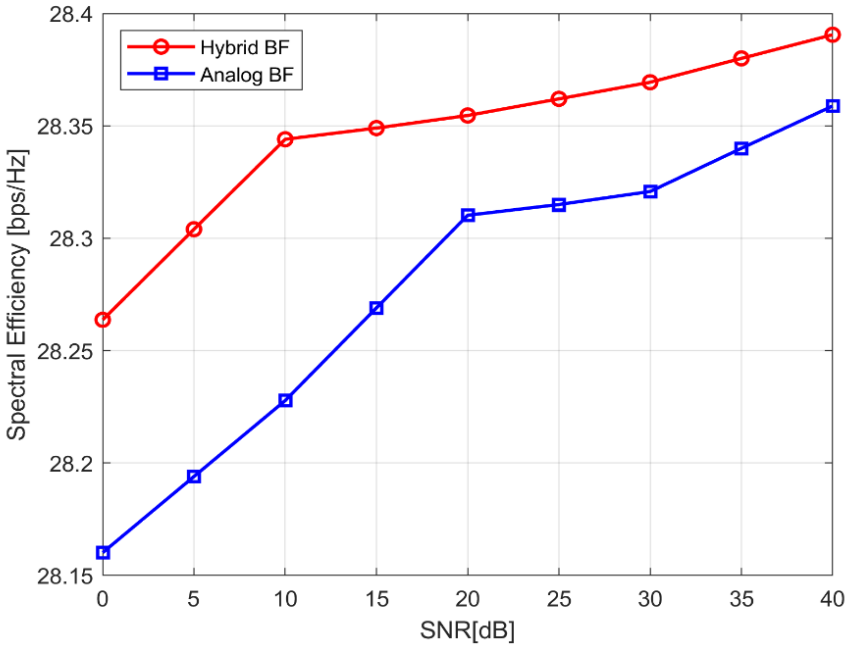

Fig. 10. Comparison of beam tracking performance based on the UKF according to the beamforming type (SE).

Figs. 8, **9**, and **10** show the FER, throughput, and SE, respectively, based on analog and hybrid beamforming. When simulating the SNR in intervals of 5 dB, from 0 dB to 40 dB, it was observed that for hybrid beamforming, the performance improved compared to that of analog beamforming.

Analog beamforming is a method of adjusting the phase by generating only one beam at a time using one RF chain. Although this approach is good in terms of hardware implementation, it has the disadvantage of being too expensive as well as limited to one user and one stream. On the other hand, hybrid beamforming is a method of simultaneously adjusting the phase of the baseband using multiple RF chains and digital signal processing of the baseband, and analog and digital beamforming are applied at the same time. Since a small number of phase regulators can be used to adjust the balance between the spectral and hardware efficiencies, we can predict better performance than with analog beamforming.

5. Conclusion

This study proposes a UKF-based beam tracking method using hybrid beamforming in a UAV-enabled NR MIMO-OFDM system. The proposed algorithm uses a nonlinear measurement function at several sample points called sigma points to estimate the motion state of the UAV as a Gaussian distribution while tracking the beam angle. In addition, by utilizing hybrid beamforming, the proposed method can be applied to multi-user and multi-stream environments over existing algorithms that are limited to single-user and single-stream environments, thus increasing the data capacity and utilization in 5G systems. The simulation results confirm that the proposed algorithm can track channel angles accurately with high spectral efficiency at the transceiver. The future research challenges include evaluating the performance of the algorithm by applying it to multi-user and multi-stream environments [12].

References

[1] M. Mozafari, W. Saad, M. Benis, Y. H. Nam, M. Debbah, “A tutorial on UAVs for wireless networks: Applications, challenges, and open problems,” *IEEE Commun. Surveys Tuts.*, vol.21, no.3, pp.2334-2360, Mar. 2019. Article (CrossRef Link)

[2] B. Li, Z. Fei, Y. Zhang, “UAV communications for 5G and beyond: Recent advances and future trends,” *IEEE Internet of Things Journal*, vol.6, no.2, pp.2241-2263, Apr. 2019. Article (CrossRef Link)

[3] [3] M. Xiao, S. Mumtaz, Y. Huang, L. Dai, Y. Li, M. Matthaiou, G. K. Karagiannidis, E. Bjornson, K. Yang, C. I, A. Ghosh, "Millimeter wave communications for future mobile networks," *IEEE Journal on Selected Areas in Communications*, vol.35, no.9, pp.1909-1935, Sep. 2017. Article (CrossRef Link)

[4] 3GPP TR 38.901 V16.1.0, "Study on channel model for frequencies from 0.5 to 100 GHz (Release 16)," 3rd Generation Partnership Project, 2019.

[5] H. L. Song, Y. C. Ko, J. G. Cho, C. H. Hwang, “Beam Tracking Algorithm for UAV Communications Using Kalman Filter,” in *Proc. of 2020 International Conference on Information and Communication Technology Convergence (ICTC)*, pp. 1101-1104, Oct. 2020. Article (CrossRef Link)

[6] W. Tan, S. D. Assimonis, M. Matthaiou, Y. Han, X. Li, S. Jin, "Analysis of different planar antenna arrays for mmWave massive MIMO systems," in *Proc. of 2017 IEEE 85th Vehicular Technology Conference (VTC Spring)*, pp.1-5, Jun. 2017. Article (CrossRef Link)

[7] J. Zhao, F. Gao, L. Kuang, Q. Wu, W. Jia, “Channel tracking with flight control system for UAV mmWave MIMO communications,” *IEEE Commun. Lett.*, vol. 22, no. 6, pp.1224–1227, Apr. 2018. Article (CrossRef Link)

[8] S. Rangan, T. S. Rappaport, E. Erkip, “Millimeter-wave cellular wireless networks: Potentials and challenges,” *Proceedings of the IEEE*, vol. 102, no. 3, pp.366–385, Mar. 2014. Article (CrossRef Link)

[9] S. M. Moon, I. T. Hwang, "Hybrid precoding with power allocation for NR MIMO-OFDM systems," in *Proc. of 2019 Eleventh International Conference on Ubiquitous and Future Networks (ICUFN)*, pp. 278-282, Jul. 2019. Article (CrossRef Link)

[10] E. A. Wan, R. Van Der Merwe, "The unscented Kalman filter for nonlinear estimation," in *Proc. of the IEEE 2000 Adaptive Systems for Signal Processing, Communications, and Control Symposium (Cat. No.00EX373)*, pp. 153-158, Oct. 2000. Article (CrossRef Link)

[11] Y. Ge, Z. Zeng, T. Zhang, Y. Sun, "Unscented Kalman filter based beam tracking for UAV-enabled millimeter wave massive MIMO Systems," in *Proc. of 2019 16th International Symposium on Wireless Communication Systems (ISWCS)*, pp. 260-264, Oct. 2019. Article (CrossRef Link)

[12] S. M. Moon, J. Y. Kim, I. T. Hwang, "Analog and digital hybrid precoding for millimeter-wave-based MU-MIMO System," *Journal of the Institute of Electronics and Information Engineers*, vol.56, no.7, pp.3-8, 2019.

Yuna Sim received her B.S. in Electronics and Computer Engineering from Chonnam National University, Gwangju, Korea in 2022. She is currently pursuing her M.S. from the Department of ICT Convergence System Engineering, College of Engineering of Chonnam National University. Her research interests include digital communications, wireless communication systems, and next-generation mobile communications: 6G, artificial intelligence, multiple-input multiple-output systems, non-terrestrial networks, orthogonal frequency-division multiplexing, and unmanned aerial vehicles.

Seungseok Sin is pursuing his B.S. in Electronics and Computer Engineering from Chonnam National University, Gwangju, Korea and is expected to graduate in 2023. His research interests include digital communications, wireless communication systems, and next-generation mobile communications: 6G, artificial intelligence, multiple-input multiple-output systems, non-terrestrial networks, orthogonal frequency-division multiplexing, and unmanned aerial vehicles.

Jihun Cho received a B.S. degree in Aerospace Engineering from Pusan National University, Busan, Korea in 2020. He was a research engineer at Korea Institute of Aviation Safety Technology in 2020. He is currently an administration staff in the National Aviation Test Center at Korea Aerospace Research Institute, Daejeon, Korea from 2021. His research interests include digital communication, aeronautical communication systems, and next-generation mobile communication: MIMO-OFDM, NR-MIMO, and CNS-ATM.

Sangmi Moon received the B.S., M.S., and Ph.D. degrees in Electronics & Computer Engineering from Chonnam National University, Gwangju, Korea, in 2012, 2014, and 2017 respectively. She was a visiting scholar in the School of Electrical Engineering and Computer Science, Oregon State University, USA, from Sep. 2017 to Feb. 2019. She was a postdoctoral research of the Department of Electronic Engineering, Chonnam National University, Korea, from Apr. 2018 to Feb. 2021. She is currently a Professor in the Department of IT Artificial Intelligence at Korea Nazarene University, Korea from Mar. 2021. Her research interests include 3D-MIMO, 3D-Beamforming, V2X, NTN, and artificial intelligence.

Young-Hwan You received the B.S., M.S., and Ph.D. degrees in electronic engineering from Yonsei University, Seoul, Korea, in 1993, 1995, and 1999, respectively. From 1999 to 2002 he had been a senior researcher at the wireless PAN technology project office, Korea Electronics Technology Institute (KETI), Korea. Since 2002 he has been a professor of the Department of Computer Engineering, Sejong University, Seoul, Korea. His research interests lie in the field of wireless communications and signal processing with particular focus on wireless communications system design.

Cheol Hong Kim received the B.S. degree in Computer Engineering from Seoul National University, Seoul, Korea in 1998 and M.S. degree in 2000. He received the Ph.D. in Electrical and Computer Engineering from Seoul National University in 2006. He worked as a senior engineer for SoC Laboratory in Samsung Electronics, Korea from Dec. 2005 to Jan. 2007. He also worked as a Professor at Chonnam National University, Korea from 2007 to 2020. Now he is working as a Professor at School of Computer Science and Engineering, Soongsil University, Korea. His research interests include computer systems, embedded systems, mobile systems, computer architecture, low power systems, and intelligent computer systems.

Intae Hwang received a B.S. degree in Electronics Engineering from Chonnam National University, Gwangju, Korea in 1990 and a M.S. degree in Electronics Engineering from Yonsei University, Seoul, Korea in 1992, and a Ph.D. degree in Electrical & Electronics Engineering from Yonsei University, Seoul, Korea in 2004. He was a senior engineer at LG Electronics from 1992 to 2005. He is currently a Professor in the Department of Electronic Engineering and Department of ICT Convergence System Engineering at Chonnam National University, Gwangju, Korea from 2006. His research interests include digital communication, wireless communication system, and next-generation mobile communication: MIMO-OFDM, V2X, NR-MIMO, NTN, and artificial intelligence.